Global warming shifts Pacific tropical cyclone location

Tim Li[1], MinHo Kwon[1], Ming Zhao[2], Jong-Seong Kug[3], Jing-Jia Luo[4], and Weidong Yu[5]

[1]*International Pacific Research Center, University of Hawaii, Honolulu, Hawaii*
[2]*GFDL, NOAA, Princeton, New Jersey*
[3]*Korea Ocean Research and Development Institute, Korea*
[4]*Research Institute for Climate Change, JAMSTEC, Japan*
[5]*First Institute of Oceanography, State Oceanic Administration, China*

Corresponding Author:

Tim Li, International Pacific Research Center, University of Hawaii at Manoa, 1680 East-West Rd., Honolulu, HI, 96822. E-mail: timli@hawaii.edu

Abstract

A global high-resolution (~ 40km) atmospheric general circulation model (ECHAM5 T319) is used to investigate the change of tropical cyclone frequency in the North Pacific under global warming. A time slice method is used in which sea surface temperature fields derived from a lower-resolution coupled model run under the 20C3M (in which historical greenhouse gases in 20th century were prescribed as a radiative forcing) and A1B (in which carbon dioxide concentration was increased 1% each year from 2000 to 2070 and then was kept constant) scenarios are specified as the lower boundary conditions to simulate the current and the future warming climate, respectively. A significant shift is found in the location of tropical cyclones from the western to central Pacific. The shift to more tropical cyclones in the central and less in the western Pacific is not attributable to a change in atmospheric static stability, but to a change in the variance of tropical synoptic-scale perturbations associated with a change in the background vertical wind shear and boundary layer divergence.

1. Introduction

Tropical cyclones (TC) are among the most devastating weather phenomena that can affect human life and economy. How global warming will affect TC activity is a hotly debated topic [Webster et al., 2005; Emanuel, 2005; Landsea et al., 2006]. It has been long recognized that TC genesis depends on sea surface temperature (SST) because a higher SST provides TCs with high ocean thermal energy. In addition to SST, TC genesis also depends on other dynamic and thermodynamic conditions such as atmospheric static stability, humidity, perturbation strength, and vertical wind shear [Gray, 1979; Wu and Lau, 1992; Emanuel and Nolan, 2004]. Particularly in the western North Pacific, atmospheric circulation patterns rather than local SST play an important role in interannual and interdecadal timescales [Chan, 2000; Matsuura et al., 2003; Ho et al., 2004] and future projection [Yokoi and Takayabu, 2009].

TCs originate from tropical disturbances. Statistically, only a small percentage of the tropical disturbances eventually develop into TCs. With the increase of the global SST and surface moisture, it is anticipated that more TCs would develop. However, many climate models simulate a global decreasing trend of TC frequency [Sugi et al., 2002; McDonald et al., 2005; Hasegawa and Emori, 2005; Yoshimura et al., 2006; Oouchi et al., 2006; Bengtsson et al., 2007]. One explanation of the decrease of TC frequency is attributed to an increase of atmospheric static stability. This is because the global warming leads to a larger increase of air temperature in the upper troposphere than in the lower troposphere; as a result, the atmosphere becomes more stable, which suppresses the TC frequency [Sugi et al., 2002; Bengtsson et al., 2007]. If this is true and it dominates the regional change of TC frequency, then one would expect the

77 decrease of TC frequency throughout all ocean basins. However, as shown by this study,
78 there are opposite trends of TC frequency between the western and central Pacific.

79 A concept of a relative SST warming was introduced recently to explain the
80 change of basin-wide TC frequency under global warming [e.g., Swanson, 2008; Vecchi
81 et al., 2008; Knutson et al., 2008; Zhao et al. 2009, 2010]. In particular, Zhao et al.
82 [2009] found that both the present-day inter-annual variability of Atlantic hurricane
83 frequency and the inter-model spread in their simulated frequency response of
84 hurricanes to 21st century global warming projections (based on the IPCC AR4 models)
85 can be well explained by a simple relative SST index defined as the Atlantic Main
86 Development Region SST minus the global tropical mean SST. While this result
87 suggests that the large-scale dynamic and thermodynamic conditions that are relevant to
88 TC genesis are closely tied to spatial distributions of SST in the Atlantic and eastern
89 Pacific [Zhao et al., 2010], such a simple relative SST index fails in explaining the
90 change in the western Pacific. Furthermore, it is worth mentioning that the relative SST
91 concept implies the importance of changes in atmospheric circulation in response to
92 change of SST distribution in affecting future TC frequency.

93 This study investigates the cause of shift of TC genesis locations in the Pacific
94 in a warmer climate based on a high-resolution atmospheric general circulation model
95 (AGCM). In the following, we first introduce the model and numerical experiments, and
96 then we discuss the model results, with a focus on the shift of TC location and
97 associated characteristics of mean state change. Finally, we summarize the main finding
98 of this study.

99 **2. Methodology and model description**

AGCM used in this study is ECHAM5 [Roeckner et al., 2003] at a horizontal resolution of T319 (about 40-km grid). This high-resolution global model is run at Japan's Earth Simulator. SST, the lower boundary condition of the model, is derived from a lower-resolution (T63) coupled version of the model (ECHAM5/MPI-OM) [Jungclaus et al., 2006], which participated in the fourth assessment report of intergovernmental panel for climate change (IPCC-AR4). Two different climate change scenarios (20C3M and A1B) were applied. In 20C3M scenario, increasing historical greenhouse gases in 20^{th} century were prescribed as a radiative forcing. In A1B scenario, carbon dioxide concentration was increased at a rate 1% per year till it reached 720 ppm and was then kept constant. A 'time-slice' method [Bengtsson et al., 1996] was applied, in which the high-resolution AGCM is forced by SST during two 20-year periods (1980-1999 and 2080-2099). The two periods are hereafter referred to as 20C and 21C, respectively.

Following Thorncroft and Hodges [2001], TCs in the model are determined based on the following three criteria: 1) 850-hPa vorticity is greater than 1.75×10^{-6} s^{-1}, 2) warm core strength (represented by the difference between 850 and 250 hPa vorticity) exceeds 0.8×10^{-6} s^{-1}, and 3) duration time exceeds 2 days. The selection of the parameter values is based on the least square fitting of the observed TC number in northern hemisphere in 20C.

3. Results

Figure 1 shows the geographical distribution of TC genesis locations in the Pacific in the 20C and 21C simulations. In 20C, TCs form primarily over the western and eastern Pacific, similar to the distribution of the observed genesis locations [Gray,

123 1979]. In 21C, however, more TCs shift their genesis locations to the Central Pacific. As
124 seen from the difference map (Fig. 1c), there are two notable TC decrease and increase
125 regions over the Pacific. One is over the North western Pacific (NWP) and the other the
126 North central Pacific (NCP). The numbers of TCs in 21C decreases by 31% over NWP
127 but increases by 65% over NCP. Thus the high-resolution AGCM simulations illustrate
128 two opposite TC trends in NWP and NCP.

129 To demonstrate that the result above is not a specific feature of the ECHAM5
130 model and its projected SST warming pattern, we also examined the simulation results
131 from the GFDL global 50-km resolution AGCM (HiRAM2.1, for detailed model
132 description and its realistic simulation of the annual, inter-annual and decadal variations
133 of TC activity, readers are referred to Zhao et al. 2009) with an ensemble SST warming
134 pattern from 18 IPCC AR4 models [Zhao et al., 2009]. The two models have different
135 treatments in various physical parameterization schemes. For example, for convective
136 heating parameterization ECHAM5 uses a mass flux scheme while HiRAM2.1 uses a
137 modified Bretherton (2004) scheme. Figure 1d shows the difference in TC genesis
138 number between 21C and 20C from the GFDL model. An opposite TC trend can also be
139 seen between NWP and NCP, supporting the ECHAM5 result.

140 To understand the cause of this distinctive shift in TC location with global
141 warming, we diagnose in the following the dynamic and thermodynamic conditions in
142 northern summer (July – October), when a majority of TCs occur, over the NWP (5-
143 25ºN, 110ºE-160ºE) and NCP (5-25ºN, 180-130ºW) regions, respectively. First we
144 examine the change of atmospheric stability in both the regions. Figures 2a and 2b show
145 the vertical profiles of the atmospheric potential and equivalent potential temperatures

averaged over NWP and NCP. The upper-level air temperature increases at a greater rate than that at lower levels in both the regions. As the static stability is measured by the vertical gradient of the potential temperature, the result implies that the atmosphere becomes more stable under the global warming in both the regions. Due to the effect of atmospheric humidity (which increases more in the lower troposphere), the vertical gradient of equivalent potential temperature approximately remains same from 20C to 21C. This implies that the atmospheric convective instability remains unchanged in both the regions. Thus, both the static stability and the convective instability changes cannot explain the opposite trends of TC frequency between NWP and NCP.

A further analysis reveals that the fundamental cause of the opposite TC trends lies in the change of dynamic conditions. As we know, TCs originate from the tropical disturbances such as synoptic wave trains and easterly waves [e.g., Lau and Lau, 1990]. The 21C simulation shows an increased variability of synoptic-scale disturbances over the NCP region but a decreased synoptic activity over the NWP region. Here the strength of the synoptic-scale disturbances is represented by the variance of the 850-hPa vorticity field that is filtered at a 2-8 day band using Lanzcos digital filter [Duchon, 1979]. The difference map (Fig. 2c) shows a remarkable decrease of the synoptic-scale variance over (10-20N, 110-140E) but an increase of the variance in (10-20N, 180-130W). The importance of synoptic activity on future projection of TC genesis frequency was also pointed out by Yokoi and Takayabu [2009]. Thus, the decreasing trend in NWP is caused by the reduced synoptic-scale activity whereas the increasing trend in NCP is caused by the strengthening of synoptic disturbances.

We argue here that the contrast of the synoptic-scale activity between NWP and

NCP results from the change of the background vertical wind shear (Fig. 3a) and low-level divergence (Fig. 3c). It has been pointed out that the easterly shear and low-level convergence of the background mean flow favor the development of tropical disturbances [Wang and Xie, 1996; Li, 2006; Sooraj et al., 2008]. In the 20C simulation, the western Pacific and Indian monsoon regions have a prevailing easterly wind shear in association with large-scale convective heating. This easterly wind shear becomes weaker in the warming climate (Fig. 3a). The weakening of the easterly wind shear corresponds to a weakened western Pacific monsoon, as seen from Fig. 3b. The weakening of the easterly shear, along with low-level divergence to its east (Fig. 3c), further suppresses the development of tropical disturbances in NWP. In contrast, the easterly wind shear and low-level convergence in NCP are strengthened, and so is the precipitation (Fig. 3). They favor the development of TCs in NCP.

What causes the change of the vertical shear and the low-level divergence? We argue that the change of the background vertical shear and the low-level divergence is closely related to changes of the trade wind in the tropics (Fig. 3c). Many IPCC-AR4 models predict an El Nino-like warming pattern in the Pacific under the global warming climate state [Solomon et al., 2007], that is, a greater SST warming occurs in the tropical eastern and central Pacific compared to that in the tropical western Pacific. As a result, the zonal SST gradient is reduced across the tropical Pacific. The reduced zonal SST gradient decreases the trade wind [Lindzen and Nigam, 1987] and weakens the Walker circulation. Furthermore, GCM simulations with a uniform SST warming also produce a weakening of the Walker circulation, which can be understood in terms of the energy and mass balance of the ascending branch of the circulation [Held and Soden, 2006; Vecchi et al., 2006]. Therefore, both the reduced zonal SST gradient and the

193 global mean SST warming decrease the trade wind.

194 The weakening of the trades leads to, on the one hand, the decrease of the
195 boundary-layer convergence in the western Pacific monsoon region and, on the other
196 hand, the increase of the boundary convergence in NCP (Fig. 3c). The former
197 suppresses the monsoon convective heating and decreases the easterly shear in NWP,
198 whereas the latter strengthens the local boundary layer moisture convergence and
199 convective heating and thus increases the easterly wind shear in NCP.

200 **4. Summary and discussion**

201 The shift of TC location in the Pacific due to the global warming is
202 investigated using a high-resolution (~ 40km) global AGCM (ECHAM5). It is noted
203 that TC genesis number decreases significantly in the western Pacific but increases
204 remarkably in the central tropical Pacific. Such a feature is also seen in the GFDL
205 HiRAM2.1 forced with an IPCC-AR4 ensemble SST warming pattern.

206 The cause of the two opposite TC trends is investigated. As the atmospheric
207 static stability increases in both the regions under global warming, this stability control
208 mechanism cannot explain the increasing trend over the central Pacific. The major
209 factor that accounts for the distinctive opposite TC trends lies in the dynamic condition
210 in the atmosphere. It is the change of strength of synoptic disturbances that is primarily
211 responsible for the distinctive changes in the TC frequency between the western and
212 central Pacific.

213 Physical processes responsible for the distinctive TC frequency changes in the
214 warming climate are discussed below. The global warming weakens the trade winds in

the Pacific through both the effect of the uniform warming and the decrease of zonal SST gradients across the tropical Pacific. In the western Pacific, the weakened Walker circulation causes the anomalous boundary layer divergence that leads to a weakening of the western North Pacific monsoon rainfall. The weakening of the monsoon heating further causes a decrease in the background easterly shear. The decreased easterly shear and associated weakening of the low-level convergence to its east reduce the synoptic activity and thus decrease the TC genesis frequency. In contrast, in the central Pacific, an anomalous boundary layer convergence is induced due to the reduced SST gradient and higher SST. This enhances the atmospheric convection and induces the easterly shear in situ. The easterly shear and the low-level convergence favor the growth of the synoptic disturbances, resulting in a TC frequency increase in the future warming climate.

Projection on future cyclogenesis frequency is subject to a wide range of uncertainties including uncertainties in model physics and SST warming patterns [Knutson et al., 2010]. ECHAM5 tends to overestimate TC genesis frequency in the central Pacific in 20C. Thus a caution is needed to interpret the results. The shift of projected TC activity in the Pacific may pose a great threat to millions' people living in Hawaii and central Pacific islands.

Acknowledgments. This work was supported by ONR grants N000140810256 and N000141010774 and NRL grant N00173-09-1-G008 and by the International Pacific Research Center that is sponsored by the Japan Agency for Marine-Earth Science and Technology (JAMSTEC), NASA (NNX07AG53G) and NOAA (NA17RJ1230). This is

238 SOEST contribution number 8016 and IPRC contribution number 720.

239

References

Bengtsson, L., M. Botzet, and M. Esch (1996), Will greenhouse gas-induced warming over the next 50 years lead to higher frequency and greater intensity of hurricanes? *Tellus*, **48A**, 57-73.

Bengtsson, L., K. I. Hodges, M. Esch, N. Keenlyside, L. Komblush, J. J. Luo, and T. Yamagata (2007), How many tropical cyclones change in a warmer climate. *Tellus*, **59A**, 539-561.

Bretherton, C.S., J.R. McCaa, and H. Grenier, 2004: A new parameterization for shallow cumulus convection and its application to marine subtropic cloud-topped boundary layers. Part I: description and 1D results. *Mon.Wea.Rev.*, 132, 864-882.

Chan, J. C. L., 2000: Tropical cyclone activity over the Western North Pacific associated with El Niño and La Niña events. *J. Climate*, **13**, 2960-2972.

Duchon, C. E. (1979), Lanczos filtering in one and two dimensions, *J. Appl. Meteoro.*, **18**, 1016-1022.

Emanuel, K. A., and D. S. Nolan (2004), Tropical cyclone activity and global climate. *In: Proc. of 26th Conference on Hurricanes and Tropical Meteorology, pp. 240-241., American Meteorological Society, Miami, FL.*

Emanuel, K.A. (2005), Increasing destructiveness of tropical cyclones over the past 30

years. *Nature*, **436**, 686-688.

Gray, W. M. (1979), Hurricanes: Their formation, structure and likely role in the tropical circulation. *Meteorology over the Tropical Oceans, D.B. Shaw (Ed.), Royal Meteorological Society*, 155–218.

Hasegawa, A., and S. Emori (2005), Tropical cyclones and associated precipitation over the western North Pacific: T106 atmospheric GCM simulation for present-day and doubled CO2 climates. *Scientific Online Letters on the Atmosphere*, **1**, 14 5–148.

Held, I. M. and B. J. Soden, (2006), Robust responses of the hydrological cycle to global warming. *J. Climate*, 19, 5686--5699.

Ho, C.-H., J.-J. Baik, J.-H. Kim, D.-Y. Gong, and C.-H. Sui, 2004: Interdecadal changes in summertime typhoon tracks. *J. Climate*, **17**, 1767-1776

Jungclaus, H., and coauthors (2006), Ocean circulation and tropical variability in the co upled model ECHAM5/MPO-OM. *J. Clim.*, **19**, 3952-3972.

Knutson, T., J. Sirutis, S. Garner, G.A.. Vecchi and I.M.Held (2008), Simulated reduction in Atlantic hurricane frequency under twenty-first-century warming condition. *Nature Geoscience*, doi:10.1038/ngeo202.

Landsea, C. W., B. A. Harper, K. Hoarau, and J. A. Knaff (2006), Can we detect trends

in extreme tropical cyclones? *Science*, **313**, 452-454.

Lau, K.-H., and N.-C. Lau (1990), Observed structure and propagation characteristics of tropical summertime synoptic-scale disturbances. *Mon. Wea. Rev.*, **118**, 1888–1913.

Li, T. (2006), Origin of the Summertime Synoptic-Scale Wave Train in the Western North Pacific. *J. Atmos. Sci.*, **63**, 1093-1102.

Lindzen, R.S., and S. Nigam (1987), On the role of sea surface temperature gradients in forcing low level winds and convergence in the tropics. *J. Atmos. Sci.*, **44**, 2440-2458.

Matsuura, T., M. Yumoto, and S. Iizuka, 2003: A mechanism of interdecadal variability of tropical cyclone activity over the western North Pacific. *Clim. Dyn.*, **21**, 105-117.

McDonald, R. E., and coauthors (2005), Tropical storms: Representation and diagnosis in climate models and the impacts of climate change. *Clim. Dyn.*, **25**, 19–36.

Oouchi, K., and coauthors (2006), Tropical cyclone climatology in a global-warming climate as simulated in a 20km-mesh global atmospheric model: Frequency and wind intensity analyses. *J. Meteorol. Soc. Japan*, **84**, 259–276.

Roeckner, E., and coauthors, 2003: The atmospheric general circulation model ECHAM5. Part I: Model description. Max Planck Institute for Meteorology

294 Rep. 349, 127 pp.

295 Solomon, S, and coauthors *(eds) Climate Change 2007: The Physical Science Basis*

296 *(Cambridge University Press for the Intergovernmental Panel on Climate Change,*

297 *2007).*

298 Sooraj, K. P., D. Kim, J.-S. Kug, S.-W. Yeh, F-F. Jin, and I.-S. Kang (2008), Effects of

299 the low frequency zonal wind variation on the high-frequency atmospheric

300 variability over the tropics. *Clim. Dyn.*, **33**, doi 10.1007/s00382-008-0483-6 (CA).

301 Sugi, M., A. Noda, and N. Sato (2002), Influence of the global warming on tropical

302 cyclone climatology: An experiment with the JMA global model. *J. Meteorol. Soc.*

303 *Japan,* **80**, 249–272.

304 Swanson, K. L., (2008), Nonlocality of Atlantic tropical cyclone intensities.

305 *Geochem. Geophys. Geosyst.*, 9, Q04V01, doi:10.1029/2007GC001844.

306 Thorncroft, C., and K. Hodges (2001), African easterly wave variability and its

307 relationship to Atlantic tropical cyclone activity. *J. Clim.,* **14**, 1166–1179.

308 Vecchi, G. A., K. Swanson, and B. Soden (2008), Whither hurricane activity.

309 *Science*, 322, 687-689.

310 Vecchi, G. A., B. J. Soden, A. T. Wittenberg, I. M. Held, A. Leetmaa and M. J.

311 Harrison (2006), Weakening of tropical Pacific atmospheric circulation due

312 to anthropogenic forcing. Nature 441, 73-76.
313 Wang, B., and X. Xie (1996), Low-frequency equatorial waves in sheared zonal flow.
314 Part I: Stable waves. *J. Atmos. Sci.*, **53**, 449–467. (1996).
315 Webster, P. J., G. J. Holland, J. A. Curry, and H.-R. Chang (2005), Changes in tropical
316 cyclone number, duration, and intensity in a warming environment. *Science*, **309**,
317 1844-1846.
318 Wu, G., and N.-C. Lau (1992), A GCM simulation of the relationship between tropical-
319 storm formation and ENSO. *Mon. Wea. Rev.,* **120**, 958-977.
320 Yokoi, S., and Y. N. Takayabu, 2009: Multi-model projection of global warming impact
321 on tropical cyclone genesis frequency over the Western North Pacific. J. Meteor.
322 Soc. Japan, 525-538.
323 Yoshimura, J., M. Sugi, and A. Noda (2006), Influence of greenhouse warming on
324 tropical cyclone frequency. *J. Meteorol. Soc. Japan,* **84**, 405–428.
325 Zhao, M., I. M. Held, S.-J. Lin and G. A.Vecchi (2009), Simulations of global
326 hurricane climatology, interannual variability, and response to global
327 warming using a 50km resolution GCM. J. Climate, 22, 6653-6678.
328 Zhao, M., I. M. Held and G. A. Vecchi (2010), Retrospective forecasts of the
329 hurricane season using a global atmospheric model assuming persistence of

SST anomalies. *Mon. Wea. Rev.*, in press.

Figure Legends

Figure 1 TC genesis number at each 2.5°x2.5° box for a 20-year period derived from T319 ECHAM5 for (a) 20C, (b) 21C, and (c) difference between (b) and (a) (21C-20C). In (c) red (orange) shaded areas indicate 95% (90%) confidence level. (d) same as (c) except from the GFDL HiRAM2.1 model with an ensemble SST pattern averaged from 18 IPCC-AR4 models (dashed line denotes the 95% confidence level).

Figure 2 Vertical profiles of potential and equivalent potential temperatures (unit: K) at 20C and 21C averaged over (a) NWP and (b) NCP and the variance difference (c) of synoptic-scale (2-8-day) vorticity at 850 hPa (unit: 10^{-10} s^{-2}) in northern summer (July-October) between 21C and 20C, with shaded areas indicating a 95% confidence level or above (with an F test).

Figure 3 Difference (21C – 20C) fields of (a) the vertical shear of zonal wind (200 hPa minus 850 hPa, unit: m s^{-1}), (b) precipitation (unit: mm day^{-1}), and (c) velocity potential (unit: s^{-1}) and wind (unit: m s^{-1}) at 850 hPa during northern summer (July-October). Areas that exceed the 95% confidence level (Student's *t* test) are shaded (for contour) and plotted (for vector).

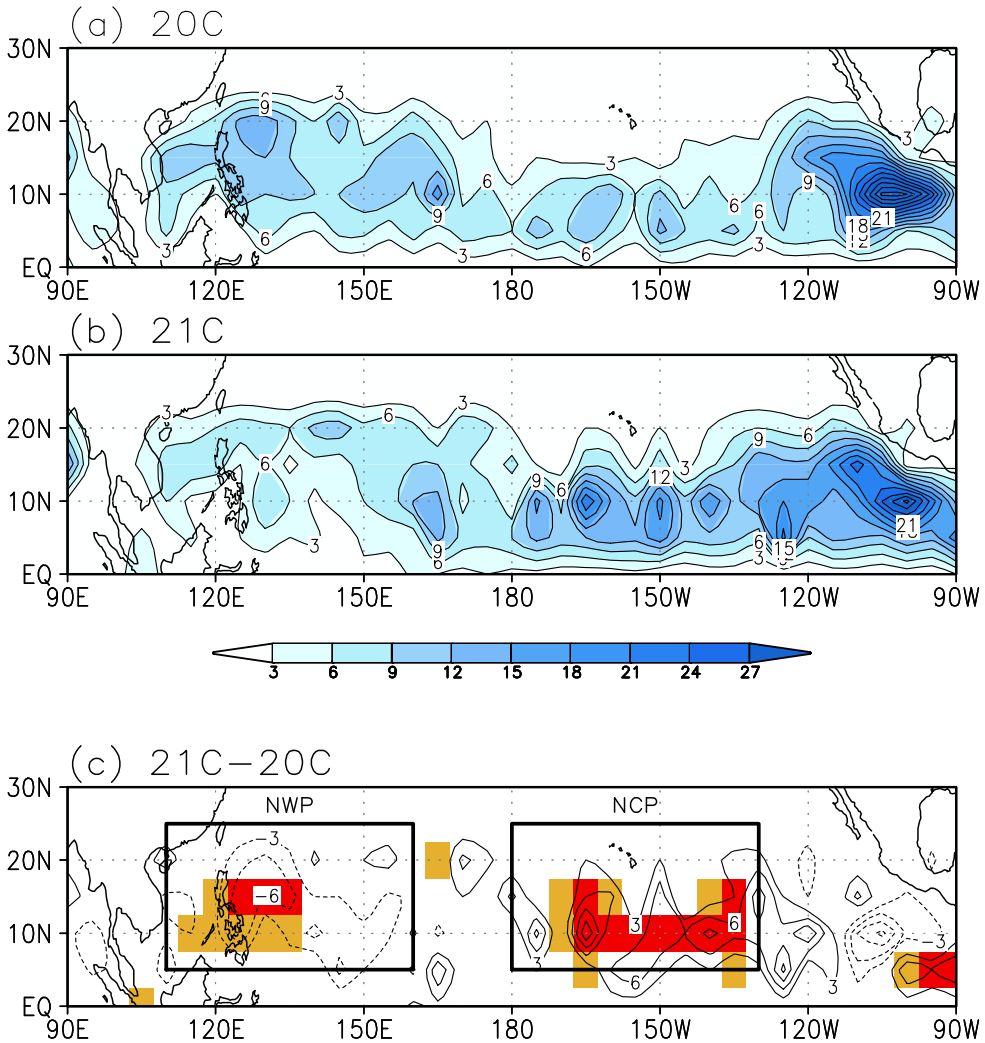

(d) 21C-20C from GFDL HiRAM2.1

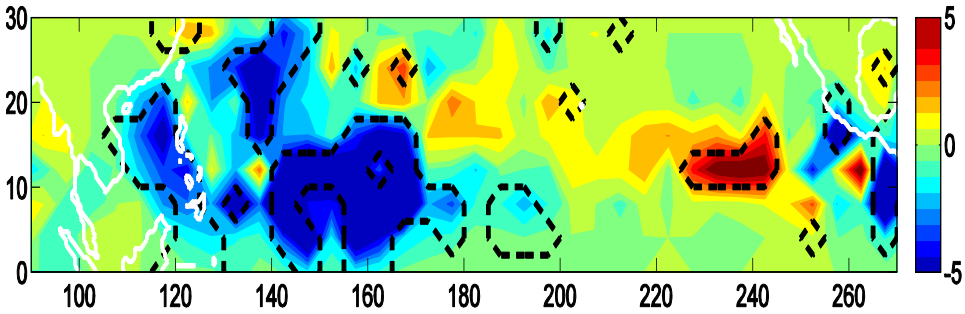

Figure 1

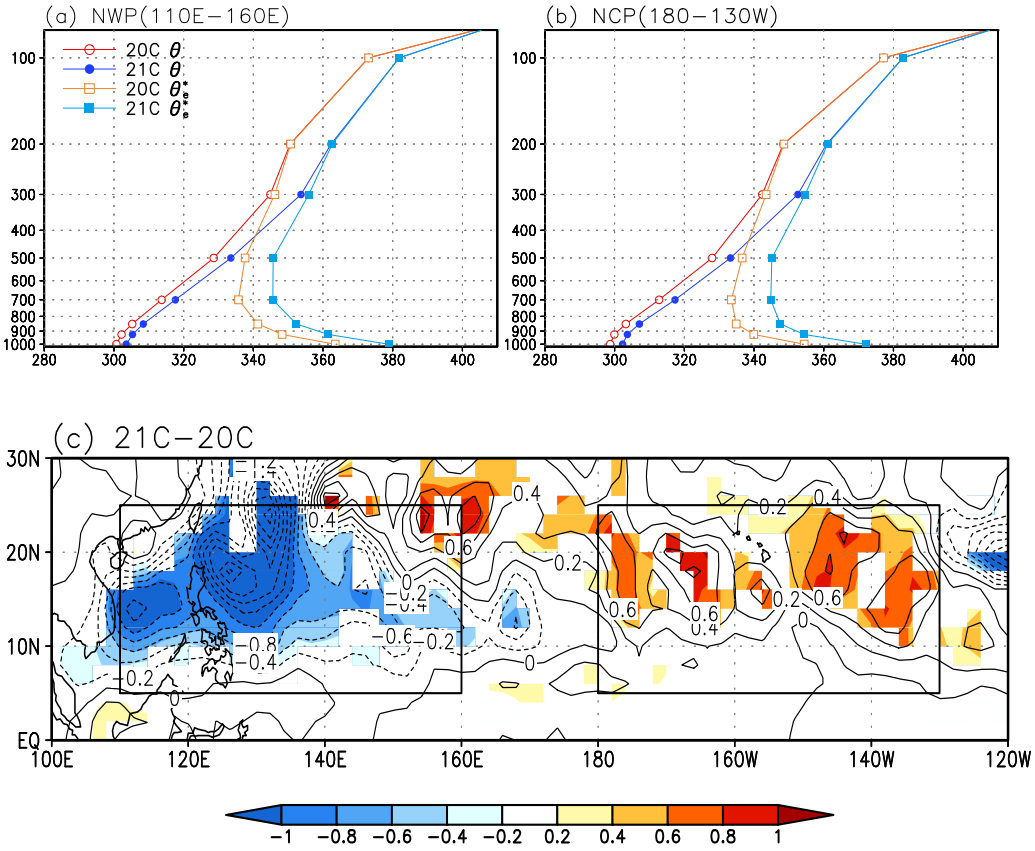
(a) NWP(110E−160E)
(b) NCP(180−130W)
20C θ
21C θ
20C θe*e
21C θe*e
(c) 21C−20C
30N
20N
10N
EQ
100E
120E
140E
160E
180
160W
140W
120W
−1 −0.8 −0.6 −0.4 −0.2 0.2 0.4 0.6 0.8 1

Figure 2

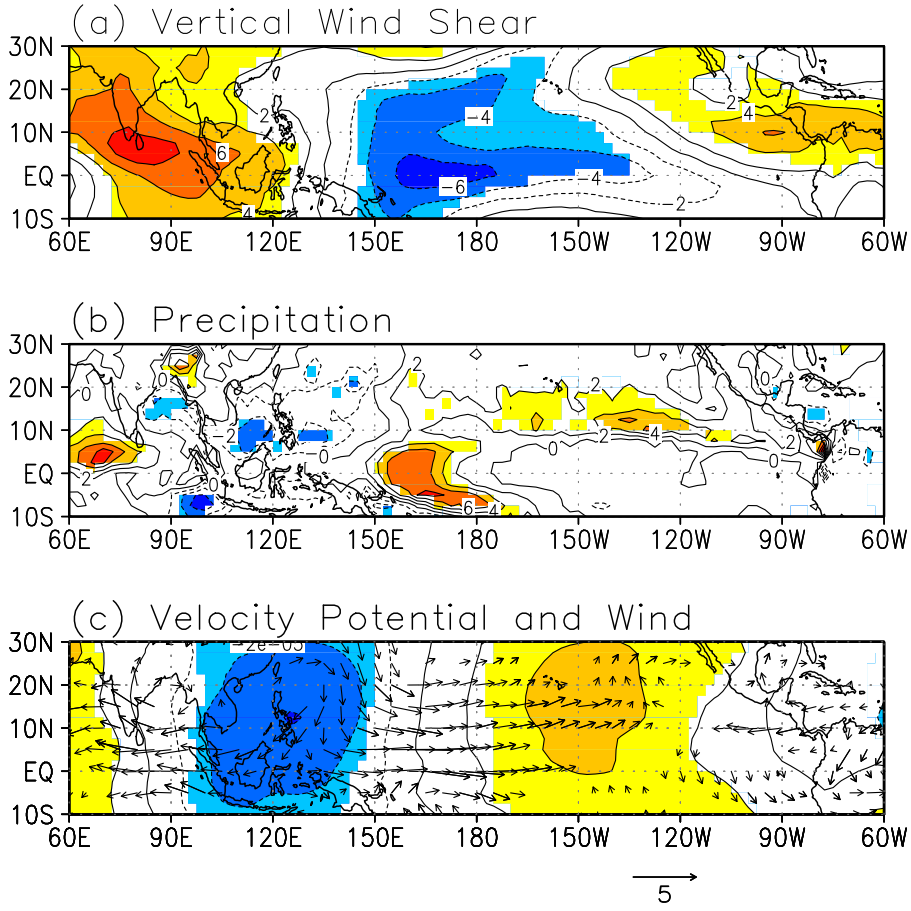

363

364 Figure 3

365